Article

Not peer-reviewed version

Alkaloid-Based Isoxazolylureas: Synthesis and Effect in Combination With Anticancer Drugs on the c6 Rat Glioma Model

Gulim K. Mukusheva , Roza I. Jalmakhanbetova , Altynay Zh. Shaibek , Manshuk S. Nurmaganbetova , Aigerym R. Zhasymbekova , Oralgazy A. Nurkenov , Ekaterina A. Akishina * , Irina A. Kolesnik , Evgenij A. Dikusar , Tatiana I. Terpinskaya , Vladimir A. Kulchitsky , Vladimir I. Potkin , Alexander L. Pushkarchuk , Dmitry A. Lyakhov , Dominik L. Michels

Posted Date: 23 May 2024

doi: 10.20944/preprints202405.1552.v1

Keywords: anabasine; cytisine; ureas; isoxazole; cytotoxic activity; antiproliferative activity; drug synergism; quantum chemical modeling molecular dockin

Article

Alkaloid-Based Isoxazolylureas: Synthesis and Effect in Combination with Anticancer Drugs on the C6 Rat Glioma Model

Gulim K. Mukusheva [1], Roza I. Jalmakhanbetova [2], Altynay Zh. Shaibek [1], Manshuk S. Nurmaganbetova [1], Aigerym R. Zhasymbekova [1], Oralgazy A.Nurkenov [3], Ekaterina A. Akishina [4,*], Irina A. Kolesnik [4], Evgenij A. Dikusar [4], Tatiana I. Terpinskaya [5], Vladimir A. Kulchitsky [5], Vladimir I. Potkin [4], Alexander L. Pushkarchuk [4], Dmitry A. Lyakhov [6] and Dominik L. Michels [6]

[1] Karaganda Buketov University, Karaganda 100024, Kazakhstan; mukusheva1977@list.ru (G.K.M.); altu_ekosya@mail.ru (A.Zh.S.); manshuk_nur@mail.ru (M.S.N.); aigera-93-93@mail.ru (A.R.Z.)
[2] L.N. Gumilyov Eurasian National University, 010000 Astana, Kazakhstan; rozadichem@mail.ru (R.I.J.)
[3] Institute of Organic Synthesis and Coal Chemistry of the Republic of Kazakhstan, Karaganda 100008, Kazakhstan; nurkenov_oral@mail.ru (O.A.N.)
[4] Institute of Physical Organic Chemistry, National Academy of Sciences of Belarus, 220072 Minsk, Belarus; irynakolesnik93@gmail.com (I.A.K.); evgen_58@mail.ru (E.A.D.); potkin@ifoch.bas-net.by (V.I.P.); alexp51@bk.ru (A.L.P.)
[5] Institute of Physiology, National Academy of Sciences of Belarus, 220072 Minsk, Belarus; terpinskayat@mail.ru (T.I.T.); kulchitski48@mail.ru (V.A.K.)
[6] Computer, Electrical and Mathematical Science and Engineering Division, King Abdullah University of Science and Technology, Thuwal 23955-6900, Saudi Arabia; dmitry.lyakhov@kaust.edu.sa (D.A.L.); dominik.michels@kaust.edu.sa (D.L.M.)
* Correspondence: che.semenovaea@mail.ru; Tel.: +375(17)3971600

Abstract: Alkaloid-based urea derivatives were produced with high yield through the reaction of anabasine and cytisine with isoxazolylphenylcarbamates in boiling benzene. Their antitumor activity in combination with the commonly used five anticancer drugs namely cyclophosphane, fluorouracil, etoposide, cisplatin, ribomustine with different mechanisms of action was investigated. Based on the quantum chemical calculations data and molecular docking, hypotheses have been put forward to explain their mutual influence when affecting on the C6 rat glioma model cells.

Keywords: anabasine; cytisine; ureas; isoxazole; cytotoxic activity; antiproliferative activity; drug synergism; quantum chemical modeling; molecular docking

1. Introduction

Cancer is one of the leading causes of death worldwide. Chemotherapy has been widely used as the primary therapy particularly against inoperable cancer or as an adjunct therapy before or after another treatment. However, it is usually accompanied with negative side effects. The combination of classical anticancer drugs with synergistic adjuvants makes it possible to reduce the therapeutic dose and thereby reduce the toxicity of chemotherapy. Therefore, the approach of using synergistic adjuvants is being seriously considered. This strategy is based on the susceptibility of different molecular pathways involved in the genesis of a particular disease to the different mechanism of action of each individual drug to improve treatment efficacy and reduce the development of drug resistance [1,2].

The main goal when developing a drug combination is to achieve an effect significantly greater than the additive effect of the individual drugs, thereby reducing dosage and toxicity. On the other hand, many types of complementary medicines may be ineffective. Worse, they can produce unintended adverse side effects or alter the actions of conventional medical treatments by inhibiting or amplifying their effects to dangerous levels [3,4]. Therefore, the search for new effective

 doi:10.20944/preprints202405.1552.v1

chemotherapeutic drugs combinations and the study of the mechanisms underlying their mutually influencing processes seem to be an urgent task of medicinal chemistry.

The isoxazole ring is often used as a central core of compounds with anticancer effects acting as inhibitor of numerous targets including aromatase, tyrosine kinase, thymidylate, ERα, PLA2, HDAC, HER2, HSP90 inhibition and apoptosis induction [5–7]. The structural features of isoxazole make it possible for multiple non-covalent interactions, especially hydrogen bonds (hydrogen bond acceptor N and O), π-π stacking (unsaturated five-membered ring) and hydrophilic interactions [8]. The authoring team of the article has been conducting research on molecular design of structures, synthesis and biotesting of new synergistic adjuvants in compositions with first-line anticancer drugs for a number of years. As a result, it was found that some isoxazole derivatives are promising candidates for synergist's role [9–11]. Previously conducted quantum chemical calculations of structural and electronic changes occurring in the cisplatin-adjuvant system based on morpholinium and 4-methylpiperazinium 4,5-dichloroisothiazol-3-carboxylates allowed us to assume that synergistic effect appeared due to conjugation of cisplatin with adjuvant through the relocation of frontier molecular orbitals as well as increase of conjugate's dipole moment what leads to change of the interaction character with cellular target and increase of the bioactivity of the system [12].

Continuing our research in this area, we expand the scope of such studies to include other chemotherapy drugs that are used in modern oncology, as well as new promising 1,2-azole derivatives possessing synergistic effects.

2. Results and Discussion

2.1. Chemistry

We previously discovered that some azolylcarbamides and carbamates can exhibit a synergistic effect in compositions with antitumor substances [13]. In this work, to obtain 5-arylisoxazolyl ureas with alkaloids fragments an approach we used in [11] was chosen. (Scheme 1). The starting 5-phenylisoxazolylcarbamate was synthesized by the reaction of 5-phenylisoxazole-3-carbonyl azide with phenol, as described by us before [11]. Isoxazolylphenylcarbamates were further introduced in the reaction with cytisine and anabasine to obtain **1-3** in 87–94% yields.

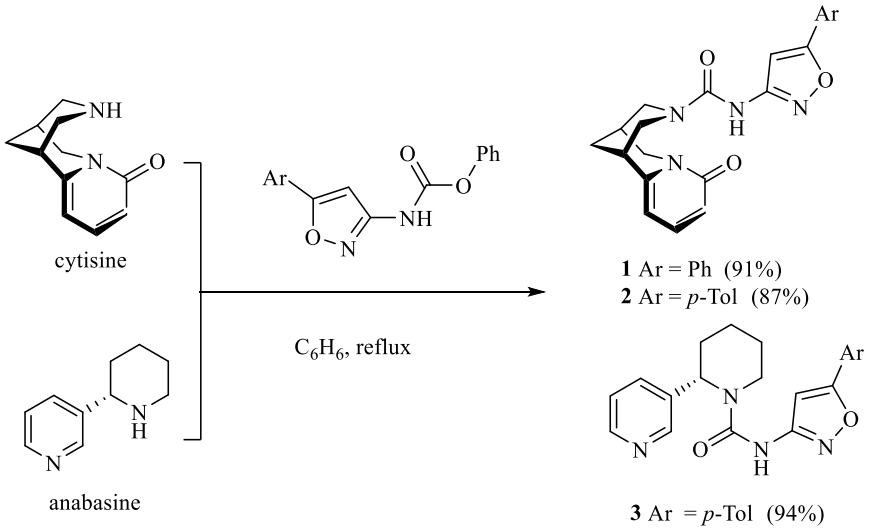

Scheme 1. Synthesis of anabasine and cytisine ureas with isoxazole fragments.

2.2. Evaluation of antitumor activity

Determination of anticancer activity of isoxazolylureas **1-3**, drugs and their binary mixtures on rat glioma cell line was carried out using flow cytometry analysis. C6 cell line is considered to be a safe and popular glioma model in the literature, providing a good simulation of glioblastoma multiforme [14].

 doi:10.20944/preprints202405.1552.v1

At the beginning the antitumor effect of synthesized isoxazolylureas was studied. The compounds **1-3** are found to have a little effect on the viability of C6 glioma cells (Fig. 1a). Suppression of cell proliferation was observed: the drugs reduced the number of cells in the samples by 19, 23 and 6% compared to the control (Figure 1b). The total number of live cells in the samples decreased by 19, 25 and 8%, respectively (Figure 1c). Thus, the anticancer effect of isoxazolylureas **1-3** is determined mainly by the antiproliferative action of the compounds. Alkaloids anabasine and cytisine in doses of 100–500 μM have a weak inhibitory effect on cells or have no effect.

Hence, even at such a fairly high dose, compounds **1-3** exhibit weak cytotoxicity along with an antiproliferative effect on tumor cells. This makes them suitable candidates for the role of low-toxic synergists of anticancer drugs.

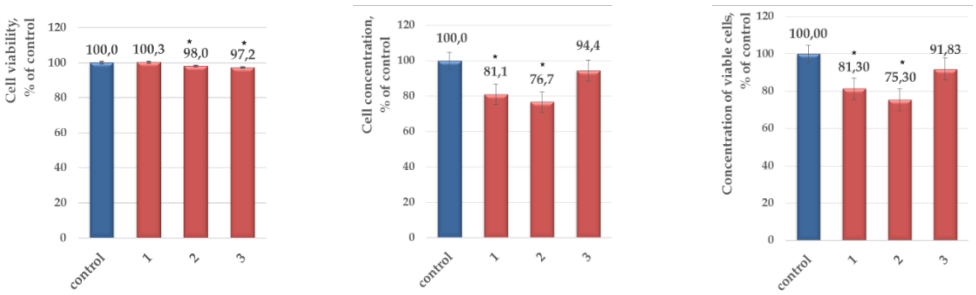

a) b) c)

Figure 1. Effect of **1-3** (200 μM) on the viability (a), concentration (b) and concentration of viable cells (c) of C6 glioma, *p < 0.05.

To study the synergistic effect the commonly used five anticancer drugs namely cyclophosphamide (CP), fluorouracil (FU), etoposide (ET), cisplatin (CPt), ribomustine (RM) with different mechanisms of action were taken (Figure 2).

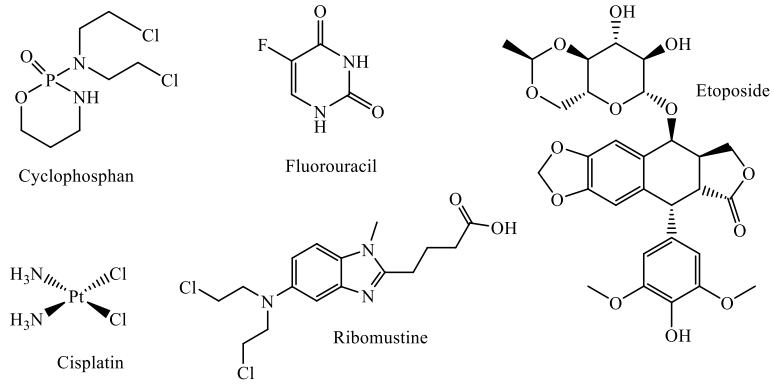

Figure 2. Anticancer drugs under study.

The cyclophosphamide (CP) is a DNA-alkylating agent which is administered as a prodrug activated by a liver cytochrome P450-catalyzed 4-hydroxylation reaction that yields the active, cytotoxic metabolite. The primary metabolite, 4-hydroxycyclophosphamide, equilibrates with the ring-open aldophosphamide that undergoes β-elimination to yield the therapeutically active DNA cross-linking phosphoramide mustard and the byproduct acrolein [15]. Tumor cells can also express P450 enzymes involved in the metabolism of cyclophosphamide [16,17]. This may provide local activation of this drug in the tumor. A number of studies have demonstrated the suppression of the growth of tumor cells of various lines in vitro under the influence of cyclophosphamide [18–20].

5-FU is known to have anticancer effects due to its metabolic transformation to 5-fluoro-deoxyuridine monophosphate and 5-fluorouridine triphosphate which are able to inhibit thymidylate synthase and incorporate into nucleic acids instead of uracil, leading to inhibition of tumor cell growth. [21,22].

 doi:10.20944/preprints202405.1552.v1

The primary mode of action of etoposide (ET) is the inhibition of the enzyme topoisomerase II function. It stabilizes DNA-enzyme complex, and accumulation of this complex enhances the probability of double-stranded DNA breaks [23].

The cisplatin (CPt) action attributed primarily to its ability to crosslink DNA purine bases, thus interfering with DNA repair mechanisms, causing DNA damage, and subsequently inducing apoptosis in cancer cells [24].

Ribomustine (RM) also acts as an alkylating agent causing intra-strand and inter-strand cross-links between DNA bases [25].

The antitumor activity of combinations at fixed drug and isoxazolylurea concentrations was assessed to identify the most promising binary mixture. We used drugs and isoxazolylureas at concentrations of 5 and 200μM respectively, and compared their combined effect with a tenfold increased drug dose (50μM).

The results of the study are summarized in the Table 1 and Figure 3. As can be seen from the experiment, compound **1** in combination with all drugs except ribomustine showed the effect of additive synergy, demonstrating an activity level approximately equal to that for summ of each compound separately. Compositions with isoxazolylurea **2** showed a clear example of antagonism in combination with the drugs cyclophosmamide, fluorouracil, etoposide, inhibiting the pharmacological activity of each other or at least one of the compounds and resulting in 2-3 fold decrease of antiprofilerative action compared to the sum of the effects of the two compounds. At the same time, the combination of compound **2** with cisplatin and ribomustine led to a completely opposite result: the synergistic effect was realized in a significant increase of the drugs action. The cytostatic activity of the binary mixture 1+RM (5 μM) exceeds the effect of the drug at a 10-fold increased dose (50μM) by 22%. Generally, the most pronounced synergistic effect was observed in the case of ribomustine mixtures with all synthesized compounds.

Table 1. Decrease in viable cell concentration (%) for antitumor drugs (c = 5 and 50 μM), compounds 1-3 (c = 200 μM) and their composition.

Decrease in viable cell concentration, %		Compound, c = 200 μM (0,2% DMSO)				
		1	2	3	Drug, c = 50 μM	
Drug, c = 5μM		18,7	24,7	8,2		
CP	26,6	41,0 Σ 45,3 (Ant)	22,2 Σ 51,3 (Ant)	19,3 Σ 34,8 (Ant)	CF	33,2
FU	7,2	24,0 Σ 25,9 (Add)	10,2 Σ 31,9 (Ant)	23,2 Σ 15,4 (Syn)	FU	42,3
ETP	28,20	45,0 Σ 46,9 (Add)	20,9 Σ 52,9 (Ant)	34,8 Σ 36,4 (Add)	ET	44,2
CPt	25,3	47,4 Σ 44,0 (Syn)	65,0 Σ 50,0 (Syn)	45,5 Σ 33,5 (Syn)	CP	93,0
RM	3,2	33,9 Σ 21,9 (Syn)	57,6 Σ 27,9 (Syn)	21,3 Σ 11,4 (Syn)	RM	35,7

*Σ is the sum of the effects of a single compound and drug

Preprints.org (www.preprints.org) | NOT PEER-REVIEWED | Posted: 23 May 2024 doi:10.20944/preprints202405.1552.v1

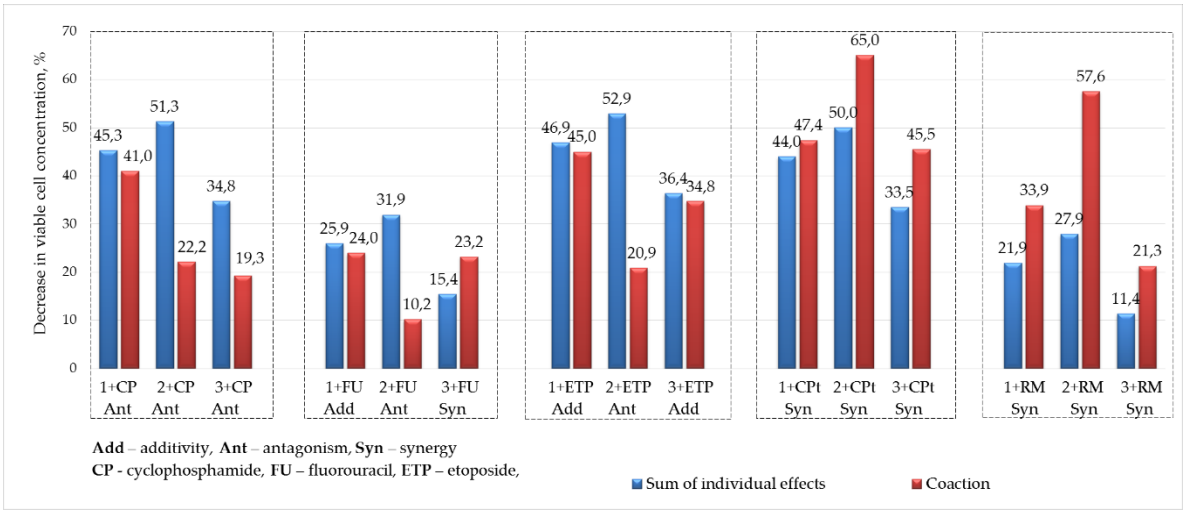

Figure 3. Decrease in viable cell concentration for binary mixtures and sum of the effects of a individual compound and drug.

The anabasine derivative **3** showed a synergistic effect with fluorouracil, cisplatin and ribomustin increasing the effectiveness of the drug by 8-12% and distinct antagonism with cyclophosphamide reducing the drug's activity by 15%. In the combination with etoposide additive action is noted.

Generally, a synergistic effect is observed to varying degrees for all ureas **1-3** when using binary mixtures with alkylating chemotherapy drugs cisplatin and ribomustine. Antagonism and the tendency to antagonism are noted for the rest drugs, except for the combination of isoxazolylurea **3** with fluorouracil.

Antagonism is known can occur through various means. The most common type is receptor antagonism, where one drug acts as an antagonist to block the effects of another drug by binding to the same receptor. This prevents the agonist drug from activating the receptor and producing its intended effect. Some drugs follow chemical antagonism, which involves the coupling of two drugs to form an inactive product, etc [26].

To interpret the observed experimental picture, quantum chemical modeling of binary drug-urea mixtures and molecular docking of isoxazolylureas were carried out, taking into account targets that determine the mechanism of drugs action.

2.3. Quantum chemical modeling

Based on the assumption that the effect of the combined action of drugs can be mediated by the formation of non-covalent drug-adjuvant conjugates as was shown before [12], we determined structural and electronic changes that occur in the system of two conjugated molecules. DFT/B3LYP-D3/cc-pvdz/LanL2DZ(Pt) level of theory was used for calculation of molecules optimal geometry, dipole moment, localization and energy characteristics of frontier molecular orbitals (FMO). Calculations were carried out both for individual compounds and their conjugates with consideration to aqueous medium, which simulates situation in living cells.

The optimized geometry of the drug-urea conjugates is presented on Figure 4, energy characteristics – in Tables 1 and 2. The energy characteristics of conjugates formation from the initial components were calculated using formula (Tables 1): $\Delta E_f = \Sigma[E_{f\ products}] - \Sigma[E_{f\ reactants}]$.

Preprints.org (www.preprints.org) | NOT PEER-REVIEWED | Posted: 23 May 2024 doi:10.20944/preprints202405.1552.v1

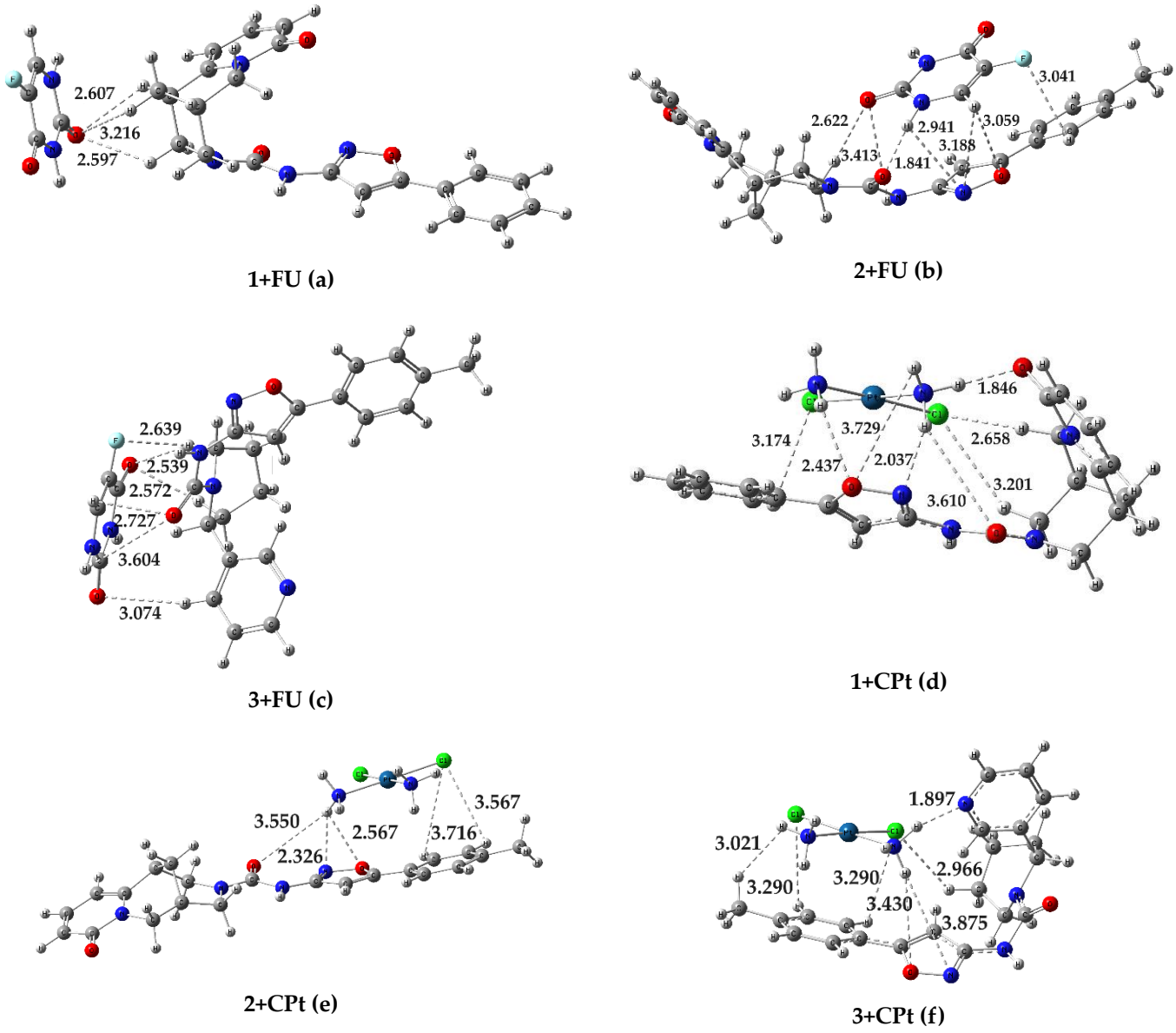

Figure 4. Calculated optimized structures with consideration to aqueous medium for conjugates **1-3** with fluorouracil and cysplatine.

It follows from calculation data that drugs molecules (**FU** and **CPt**) and ureas derivatives **1-3** form conjugates with shortened interatomic distances due to non-covalent interactions caused by hydrogen and van der Waals bonds (Figure 4a-f). As can be seen from Figure 4, the structure of isoxazolylurea **2** differs from the other two in its most linear spatial arrangement, which results in the varying degrees of conjugates stability due to the participation of different atoms in intermolecular bonds formation. Thus, in the case of fluorouracil, the most stable complex is observed with compound **2** with ΔE_f = -16.88 kcal/mol (Table 2). Hydrogen bonds are expressed between oxygen and nitrogen atom of urea fragment, nitrogen atom of isoxazole heterocycle and N-H and C=O fragment of fluorouracil $C{=}O_{urea}\cdots H\text{-}N/N_{isox}\cdots H\text{-}N/C{=}O\cdots H\text{-}N_{urea}$ with interatomic distances of 1.84, 2.94 and 3.41 Å respectively. Other non-covalent interactions represent weak unconventional C-H···O, C-H···N, C-H···F hydrogen bonds with interatomic distances 2.62-3.19 Å. The formation of conjugates **1+FU (a)** and **3+FU (c)** does not involve atoms of the isoxazole heterocycle; only weak unconventional hydrogen bonds with atoms of alkaloid fragments are generated (2.53-3.60 Å). As for conjugates with cisplatin, the opposite situation is observed: **1+CPt (d)** and **3+CPt (f)** turned out to be more stable with ΔE_f = -24.96 and -21.18 kcal/mol (Table 2). In contrast to conjugate **2+CPt (e)** the formation of hydrogen bonds involved the nitrogen atom of the pyridine heterocycle of anabasine and oxygen

 doi:10.20944/preprints202405.1552.v1

atom of cytisine C=O group in addition to the N, O atoms of the isoxazole heterocycle and the urea fragment. The above allows us to conclude that the formation of stable complexes leads to the manifestation of antagonistic effects in the drug-urea system.

Table 1. Energy characteristics of the conjugates formation process from the initial components **1–3**, **FU**, **CPt.**

Conjugate	ΔE_f, a.e.	ΔE_f, kcal/mol
1+FU	-0,009871226	-6,19
2+FU	-0,026896256	-16,88
3+FU	-0,018223976	-11,44
1+CPt	-0,03977506	-24.96
2+CPt	-0,02215013	-13.90
3+CPt	-0,03375495	-21.18

The energies of frontier molecular orbitals (FMO) often considered as important descriptors determining the biological activity of the molecule. One of the key characteristics in FMO theory are the difference between the energies of HOMO and LUMO (energy gap ΔE). The obtained values calculated using DFT/B3LYP-D3/cc-pvdz/LanL2DZ(Pt) level of theory are given in Table 2. Generally the formation of all conjugates is accompanied by a significant decrease in ΔE: when going from fluorouracil FU to conjugates the average value of decrease is 0.88 eV, from cisplatine to its conjugates – 0.37 eV. This indicates an increase in reactivity of the system, which could mean more active binding with biological sites. Worth mentioning that the decrease of ΔE for cisplatin conjugates occurs due to an increase in the HOMO energy by 0.47 eV which contributes to the realization of their nucleophilic potential.

Table 2. Theoretical electronic parameters (energies of HOMO and LUMO, energy gap ΔE,) and global reactivity descriptors for compounds **1-3**, flourouracil, cisplatin and their conjugates.

	E_{HOMO}, eV	E_{LUMO}, eV	ΔE, eV	μ (eV)	χ (eV)	η (eV)	S (eV^{-1})	ω (eV)	D, Db
1	-5.7689	-1.5192	4.2496	-3.6441	3.6441	2.1248	0.2353	3.1248	10.24
2	-5.9797	-1.4343	4.5454	-3.7070	3.7070	2.2727	0.2200	3.0232	5.24
3	-6.2992	-1.5160	4.7833	-3.9076	3.9076	2.3917	0.2091	3.1922	6.94
FU	-6.6562	-1.2798	5.3765	-3.9680	3.9680	2.6883	0.1860	2.9281	5.13
1+FU	-5.7653	-1.5241	4.2412	-3.6447	3.6447	2.1206	0.2358	3.1321	8.23
2+FU	-5.9923	-1.5347	4.4575	-3.7635	3.7635	2.2288	0.2243	3.1775	3.57
3+FU	-6.3055	-1.5206	4.7849	-3.9131	3.9131	2.3925	0.2090	3.2000	2.01
CPt	-6.5305	-1.7475	4.7830	-4.1390	4.1390	2.3915	0.2091	3.5817	15.94
1+CPt	-5.9642	-1.6504	4.3139	-3.8073	3.8073	2.1570	0.2318	3.3601	9.44
2+CPt	-5.9931	-1.6784	4.3147	-3.8358	3.8358	2.1574	0.2318	3.4100	19.75
3+CPt	-6.1966	-1.5720	4.6246	-3.8843	3.8843	2.3123	0.2162	3.2625	7.77

Global reactivity descriptors such as electronegativity (χ), chemical potential (μ), chemical softness-hardness (η and S), electrophilic index (ω) are highly successful in predicting stability properties and reactivity trends of the molecular systems. The formal definitions of all these descriptors and working equations for their computation have been described in [27]. From theoretical calculations, it was found that chemical hardness (softness) value decreases (increases) when moving from drugs to conjugates, which indicates an increase in their chemical reactivity. The values of ω for conjugates shows that the electrophilicity of binary systems with fluorouracil increases, while with cisplatin, on the contrary, it decreases (Table 2).

The work [12] provides data on the correlation between an increase in the potentiating activity of cisplatin complexes with heterocyclic compounds (having a rigid conformational structure) and an increase in the values of their calculated dipole moments in comparison with pure cisplatin. In

 doi:10.20944/preprints202405.1552.v1

this work, acylurea derivatives have the possibility of conformational rotation of C-C, C-N and N-N bonds, and no such correlation is observed.

Determination of localization of FMO is important for establishing preferred directions and regions of the molecule for attack by nucleophiles and electrophiles. Results of calculating localization of HOMO and LUMO are shown in the form of 3D isosurfaces (Figs. 5).

Formation of conjugates with fluorouracil **1+FU**, **2+FU**, **3+FU** leads to displacement of LUMO from drug molecule and its localization on isoxazole heterocycles (Figure 5). Since LUMO determines interaction with target nucleophilic sites, this type of binding will be realized through isoxazole heterocycle. Binding to electrophilic proteine sites determines localization of HOMO in conjugate. Calculations for conjugate molecules showed that HOMO in all fluorouracil conjugates is completely localized on isoxazole heterocycle or cytisine fragment but not on drug molecule. This means that the first act of interaction with the electrophilic and nucleophilic regions of protein sites is realized mainly due to the adjuvant molecule. In addition, based on previous findings, the **2+FU** complex turned out to be the most stable, which likely interfears the drug molecule own action and makes the resulting conjugate the least active against biological targets.

As for cisplatin conjugates **1+CPt** and **2+CPt** LUMO are uniformly distributed between the isoxazole heterocycle and the cisplatin molecule, and HOMO are located on the cytisine fragment. Meanwhile the cisplatin molecule is responsible for interaction with nucleophilic sites in **3-CPt** conjugate, LUMO are concentrated here on the drug molecule. In contrast to **1+CPt** and **2+CPt** conjugates HOMO in **3-CPt** do not affect the alkaloid fragment, being dispersed between cisplatin and the isoxazole heterocycle. All the given facts may indicate a coordinated mechanism of action cisplatin and the adjuvant in binary mixtures towards biological targets.

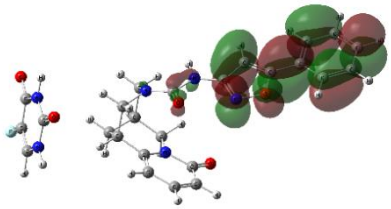

1+FU (E_{LUMO} = -1.5241 eV)

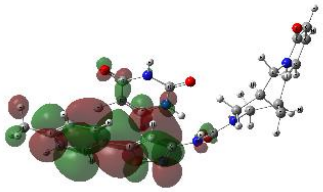

2+FU (E_{LUMO} = -1.5347 eV)

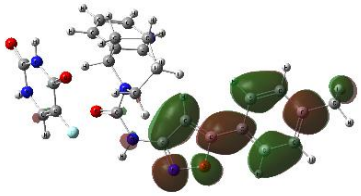

3+FU (E_{LUMO} = -1.5206 eV)

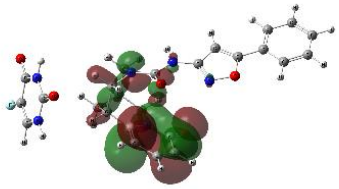

1+FU (E_{HOMO} = -5.7653 eV)

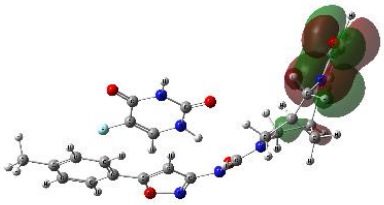

2+FU (E_{HOMO} = -5.9923 eV)

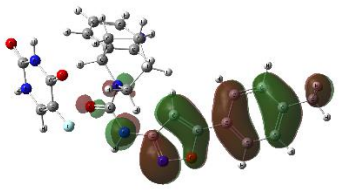

3+FU (E_{HOMO} = -6.3055 eV)

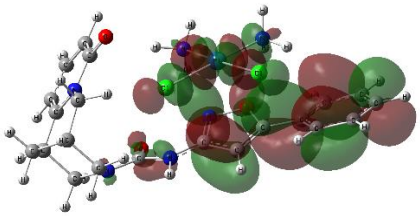

1+CPt (E_{LUMO} = -1.6504 eV)

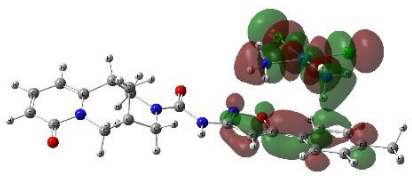

2+CPt (E_{LUMO} = -1.6784 eV)

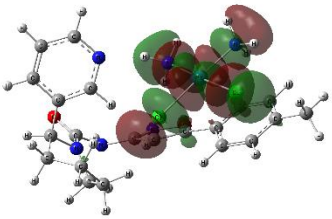

3+CPt (E_{LUMO} = -1.5720 eV)

 doi:10.20944/preprints202405.1552.v1

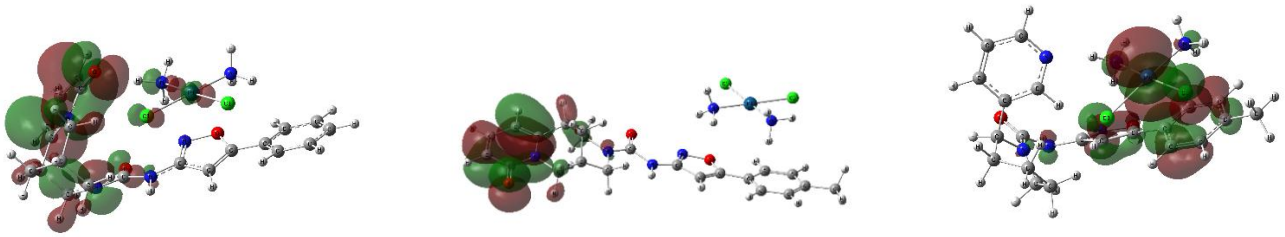

1+CPt (E_{HOMO} = -5.9642 eV) **2+CPt** (E_{HOMO} = -5.9931 eV) **3+CPt** (E_{HOMO} = -6.1966 eV)

Figure 5. Localizations of HOMO and LUMO in molecules of conjugates in the form of 3D isosurfaces with consideration to water.

2.4. Docking studies

Thymidylate synthase is one of the key enzymes in carcinogenesis and for this reason is an critical target for cancer chemotherapy. As previously noted, the main mechanism of action of fluorouracil is its conversion into 5-fluoro-2-deoxy-5-monophosphate (FdUMP) resulting in inhibition of TS and DNA synthesis. In order to study the possibility of thymidylate synthase inhibition by isoxazolyl ureas **1-3**, as a process competing with the binding of fluorouracil and its metabolite to the same target, molecular docking was carried out using software packages AutoDock/Vina 4.2.6 and CHIMERA 1.16, Biovia Discovery Studio 2024 for visualization of the docked pose. The crystal structure of target protein TS (mouse thymidylate synthase, PDB ID: 5FCT) was downloaded from the Protein Data Bank.

The efficiency of interactions was evaluated based on the changes observed in predicted binding energies and bonds formed with the active site residues of TS along with the predicted inhibition constant (K_i value) in the molecular docking analysis.

As can be seen from the Figure 6 and Table 3, all isoxazolyl ureas demonstrate a good binding degree to the thymidylate synthase protein site, forming an extensive system of residues interactions. The binding energy of the **1-3** with tymidylate synthase are -9.3, -9.9, -10.0 kcal/mol respectively, which even exceeds that for fluorouracil (-5.1 kcal/mol). Generally, ureas **1-3** form stable complexes with thymidylate synthase protein mainly due to the hydrophobic interactions of electron-rich π systems of isoxazole heterocycle and aromatic rings with aminoacid residues rather than hydrogen bonds as occurs with fluorouracil and its metabolite.

1

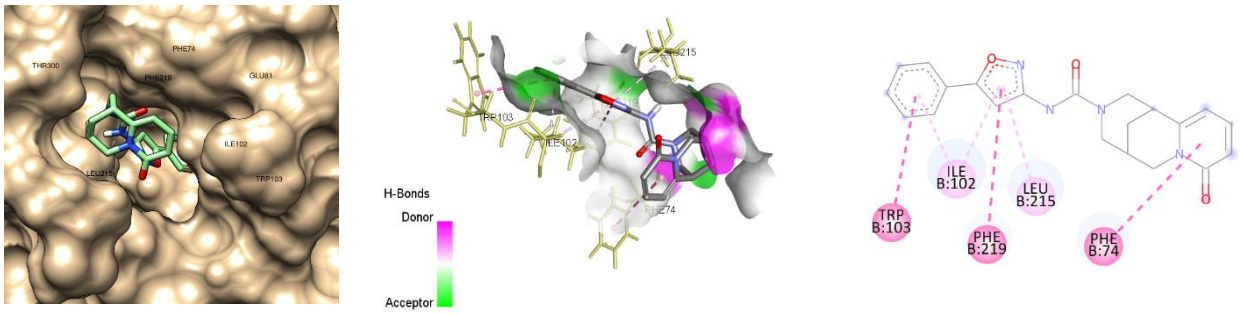

 doi:10.20944/preprints202405.1552.v1

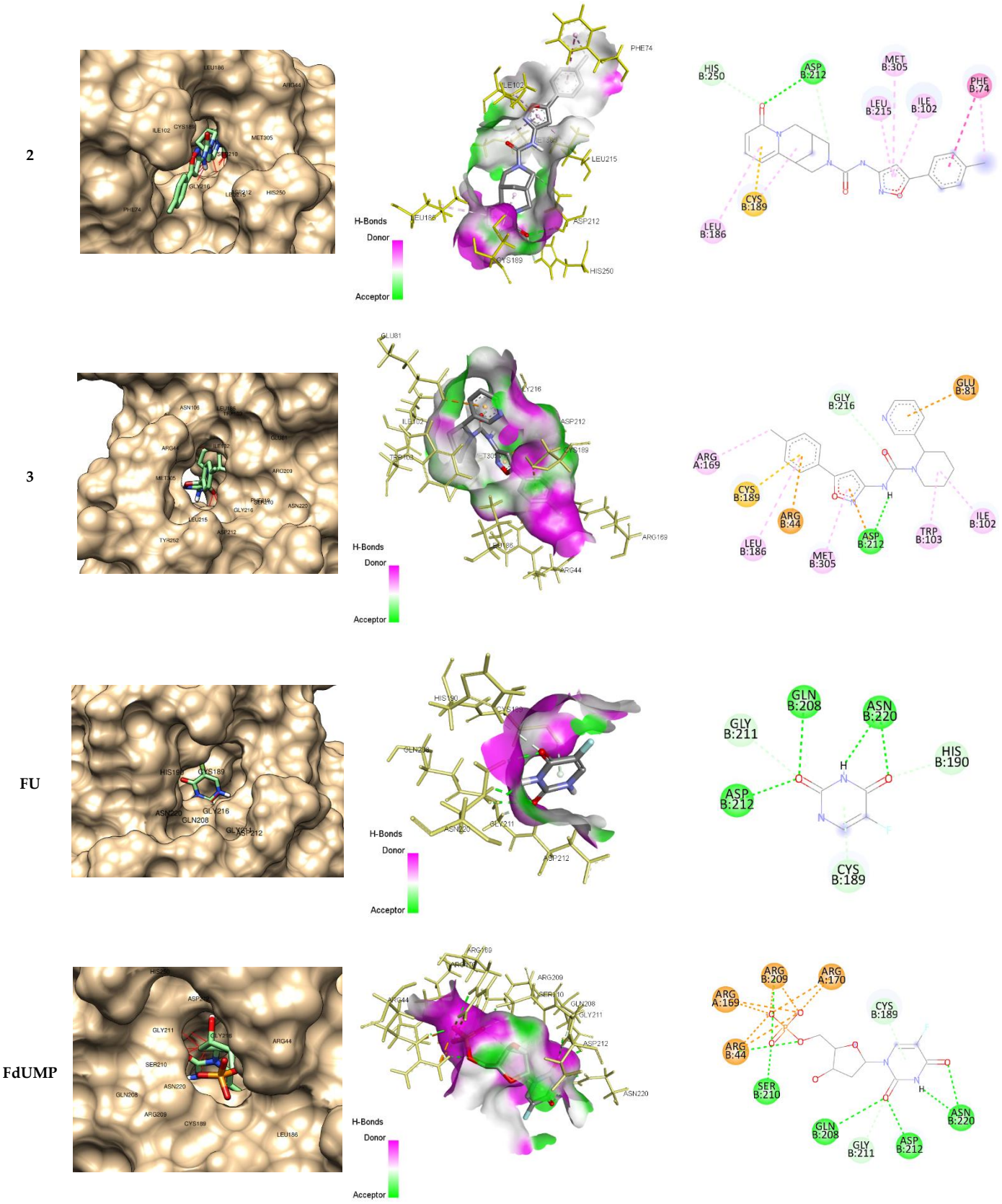

Figure 6. Binding interactions of isoxazolyl ureas **1-3** and fluorouracil **FU** and its metabolite 5-fluoro-2'-deoxyuridine-5'-monophosphate **FdUMP** with thymidylate synthase.

Table 3. Molecular docking analysis of binding **1-3, FU, FdUMP** with thymidylate synthase (PDB ID: 5FCT).

 doi:10.20944/preprints202405.1552.v1

	Binding energy, ΔG (kcal/mol)	Inhibition constant, K_i	Residues Interactions			
			Hydrogen bond	Electrostatic interactions	Hydrophobic Bond	Pi-Sulfur
1	-9.3	152 nM	0	0	6 (LEU215, PHE74, PHE219, ILE102, TRP103)	0
2	-9.9	55 nM	3 (ASP212, HIS250)	0	7 (PHE74, ILE102, LEU215, MET305, LEU186, CYS189)	1 (CYS189)
3	-10.0	47 nM	2 (ASP212, GLY216)	3 (ARG44, GLU81, ASP212)	6 (ARG169, LEU186, MET305, TRP103, ILE102)	1 (CYS189)
FU	-5.1	183 μM	8 (ASP212, GLN208, ASN220, GLY211, HIS190, CYS189)	0	0	1 (CYS189)
FdUMP	-9.5	109 nM	14 (ASN220, ASP212, GLN208, GLN211, CYS189, SER210, ARG44, ARG169, ARG170, ARG209)	8 (ARG44, ARG169, ARG209, ARG107)	0	1 (CYS189)

It is observed that the urea **2, 3** and **5-FU** and **FdUMP** occupy similar protein site forming bonds with ASN212, CYS189, ARG169, ARG44 amino acid residues (Table 3), which confirms the possibility of competing binding processes with the thymidylate synthase site. Meanwhile, for urea **1** the weakest binding is observed and besides, it interacts with other amino acid residues of the target protein.

Considering the high binding energy with TS of all ureas, molecular docking data cannot explain such a different manifestation of fluorouracil in the composition with aduvants (both antagonism and synergism are observed), probably ureas can be multitarget ligands that attack other proteins as well. Besides, summing up the data on energy characteristics of the fluorouracile-urea conjugates formation and docking data on binding energy with TS we can assume that adjuvtants will rather bind the FU into a stable complex, preventing the drug from exerting its effect (ΔE_f ranges from -6,19 to -16,88 kcal/mol), this especially applies to isoxazolylurea **2**.

3. Materials and Methods

3.1. General Chemistry Section

UV spectra were recorded on a Varian Cary 300 spectrophotometer using quartz cuvettes with l = 1 cm. The concentration of the studied compounds in methanol was 4×10^{-5}–$1\cdot10^{-4}$ M. IR spectra were registered on a Thermo Nicolet Protege 460 Fourier transform spectrometer in KBr pellets.

^{1}H and ^{13}C NMR spectra were acquired on a Bruker Avance 500 spectrometer (500 and 125 MHz, respectively) in $CDCl_3$. The residual solvent signals ($CDCl_3$, δH 7.26, δC 77.2 ppm) were used as internal standard. The assignment of signals in the ^{13}C NMR spectra was performed using the DEPT technique.

Liquid chromatography–mass spectrometry spectra were recorded on an Agilent 1200 LC-MS system with an Agilent 6410 Triple Quad Mass Selective Detector with electrospray ionization in the positive ion registration mode (MS2 scanning mode). An Agilent ZORBAX Eclipse XDB-C18 (4.6 × 50 mm, 1.8 μm) column was used. The mobile phase was MeCN–H_2O + 0.05% HCO_2H with gradient elution from 40 to 90% MeCN in 10 min. A flow rate of 0.5 mL/min was used.

Elemental analysis was performed on a Vario MICRO cube CHNS-analyzer. Melting points were determined on a Kofler bench.

The optical activity of the compounds was measured on a polarimeter MCP 100 Anton Paar.

 doi:10.20944/preprints202405.1552.v1

Reagents and solvents used were of analytical grade with the content of the main component being more than 99.5%. Phenyl (5-arylisoxazol-3-yl)carbamate were synthesized according to previously described procedures [11].

(–)-Anabasine (colorless viscous liquid, turning yellow in air and in the light; bp 276°C at 760 mmHg, 104–105°C at 2 mmHg; d_{20} 1.0455, n_D 1.5430, $[\alpha]_D^{20}$ –82°) was isolated from anabasine hydrochloride (commercial product of Shymkentbiopharm, Kazakhstan) as an individual isomer.

(–)-Cytisine (commercial product of Shymkentbiopharm, Kazakhstan) is a white crystalline substance that crystallizes from acetone in rhombic prisms, mp. 153°C, $[\alpha]_D^{20}$ = -119° (in aqueous solution).

3.1.1. General Procedure for the Synthesis of anabasine and cytisine ureas 1-3.

A mixture containing 1.6 g of anabasine (or 1.9 g of cytisine, 10 mmol) and 10 mmol of phenyl (5-arylisoxazol-3-yl)carbamate in 30 ml of benzene was boiled with stirring for 6 hours. The solvent was removed in vacuum. Diethyl ether (50 ml) was added to the oily residue and the mixture was boiled until complete crystallization. The crystalline product was separated by filtration, washed with ether and dried in air at room temperature.

(1R,5R)-8-oxo-N-(5-phenylisoxazol-3-yl)-1,5,6,8-tetrahydro-2H-1,5-methanopyrido[1,2-a][1,5]diazocine-3(4H)-carboxamide (**1**): beige solid; yield 91%; mp 241–242°C; $[\alpha]_D^{25}$ -193°; UV (MeOH c = $7\cdot10^{-5}$ M) λ_{max} (log ε): 243 (4.26), 260 (4.38), 311 (3.87); IR (KBr) ν 3313, 3180, 2933, 2867, 1692, 1653, 1623, 1595, 1576, 1539, 1424, 1341, 1265, 1222, 1187, 1102, 943, 810, 797, 770, 687 cm^{-1}; ^1H NMR ($CDCl_3$, 500 MHz) δ 1.97–2.04 (2H, m, CH_2), 2.56 (1H, s, CH), 3.10 (1H, s, CH), 3.19–3.25 (2H, m, CH_2), 3.90 (1H, dd, *J* = 15.6, 6.6 Hz, CH_2), 4.30–4.35 (2H, m, CH_2), 4.46 (1H, d, *J* = 13.00 Hz, CH_2), 6.02 ($1H_{Py}$, dd, *J* = 6.8, 0.8 Hz), 6.45 ($1H_{Py}$, dd, *J* = 9.0, 1.0 Hz), 7.07 ($1H_{isox}$, s), 7.21 ($1H_{Py}$, dd, *J* = 9.0, 6.9 Hz), 7.40–7.45 ($3H_{Ar}$, m), 7.70 ($2H_{Ar}$, dd, *J* = 8.0, 1.5 Hz), 9.25 (s, NH); ^{13}C NMR ($CDCl_3$, 125 MHz) δ 26.00 (CH_2), 27.57 (CH), 34.73 (CH), 49.05 (CH_2), 50.54 (CH_2), 51.36 (CH_2), 95.10 (CH_{isox}), 105.73 (CH_{Py}), 117.66 (CH_{Py}), 125.71 ($2CH_{Ar}$), 129.12 ($2CH_{Ar}$), 130.39 (CH_{Ar}), 139.03 (CH_{Py}), 127.58, 148.72, 154.35, 160.55, 163.62, 169.12 ($6C_{quater}$); MS *m/z* (I_{rel}, %) 377.20 $[M+H]^+$ (100); Anal. calcd. for $C_{21}H_{20}N_4O_3$ (376.41): C, 67.01; H, 5.36; N, 14.88%. Found: C, 67.22; H, 5.47; N, 14.61%.

(1R,5R)-8-oxo-N-(5-(p-tolyl)isoxazol-3-yl)-1,5,6,8-tetrahydro-2H-1,5-methanopyrido[1,2-a][1,5]diazocine-3(4H)-carboxamide (**2**): beige solid; yield 87%; mp 255–257°C; $[\alpha]_D^{25}$ -250°; UV (MeOH c = $7\cdot10^{-5}$ M) λ_{max} (log ε): 240 (4.20), 266 (4.43), 310 (3.87); IR (KBr) ν 3146, 3029, 2925, 2886, 2776, 1650, 1625, 1611, 1564, 1545, 1507, 1428, 1337, 1257, 1229, 1143, 1061, 789 cm^{-1}; ^1H NMR ($CDCl_3$, 500 MHz) δ 1.96–2.04 (2H, m, CH_2), 2.36 (s, CH_3), 2.55 (1H, s, CH), 3.09 (1H, s, CH), 3.21 (1H, d, *J* = 12.6 Hz, CH_2), 3.23 (1H, dd, *J* = 12.9, 1.9 Hz, CH_2), 3.90 (1H, dd, *J* = 15.6, 6.6 Hz, CH_2), 4.28–4.35 (2H, m, CH_2), 4.45 (1H, d, *J* = 13.00 Hz, CH_2), 6.01 ($1H_{Py}$, dd, *J* = 6.9, 1.0 Hz), 6.44 ($1H_{Py}$, dd, *J* = 9.0, 1.2 Hz), 7.02 ($1H_{isox}$, s), 7.20 ($1H_{Py}$, dd, *J* = 9.0, 6.8 Hz), 7.22 ($2H_{Ar}$, d, *J* = 8.0 Hz), 7.59 ($2H_{Ar}$, d, *J* = 8.1 Hz), 9.27 (s, NH); ^{13}C NMR ($CDCl_3$, 125 MHz) δ 21.58 (CH_3), 25.98 (CH_2), 27.55 (CH), 34.72 (CH), 49.06 (CH_2), 50.45 (CH_2), 51.33 (CH_2), 94.50 (CH_{isox}), 105.69 (CH_{Py}), 117.64 (CH_{Py}), 125.64 ($2CH_{Ar}$), 129.80 ($2CH_{Ar}$), 139.00 (CH_{Py}), 124.87, 140.70, 148.71, 154.32, 160.53, 163.60, 169.31 ($7C_{quater}$); MS *m/z* (I_{rel}, %) 391.20 $[M+H]^+$ (100); Anal. calcd. for $C_{22}H_{22}N_4O_3$ (390.44): C, 67.68; H, 5.68; N, 14.35%; Found: C, 67.91; H, 5.75; N, 14.09%.

(S)-2-(pyridin-3-yl)-N-(5-(p-tolyl)isoxazol-3-yl)piperidine-1-carboxamide (**3**): beige solid; yield 94%; mp 114–116°C; $[\alpha]_D^{25}$ -139°; UV (MeOH c = $8\cdot10^{-5}$ M) λ_{max} (log ε) 264 (4.43); IR (KBr) ν 3254, 3216, 3097, 3063, 2946, 2861, 1671, 1628, 1571, 1555, 1426, 1321, 1267, 1257, 1161, 1020, 947, 785 cm^{-1}; ^1H NMR ($CDCl_3$, 500 MHz) δ 1.48-1.61 (1H, m, CH_2), 1.64-1.80 (3H, m, CH_2), 2.02-2.13 (1H, m, CH_2), 2.39 (3H, s, CH_3), 2.39–2.46 (1H, m, CH_2), 3.00–3.11 (1H, m, CH_2), 4.11–4.20 (1H, m, CH_2), 5.74–5.82 (1H, m, CH), 7.22 ($1H_{isox}$, s), 7.24 ($2H_{Ar}$, d, *J* = 8.0 Hz), 7.30 ($1H_{Py}$, dd, *J* = 8.0, 4.7 Hz), 7.56 ($2H_{Ar}$, d, *J* = 8.8 Hz), 7.64 ($1H_{Py}$, d, *J* = 8.0 Hz), 8.51 ($1H_{Py}$, d, *J* = 4.4 Hz), 8.61 ($1H_{Py}$, d, *J* = 1.8 Hz), 9.37 (s, NH); ^{13}C ЯМР ($CDCl_3$, 125 MHz) δ 19.40 (CH_2), 21.63 (CH_3), 25.65 (CH_2), 27.88 (CH_2), 41.45 (CH_2), 51.86 (CH), 94.39 (CH_{isox}), 123.93 (CH_{Py}), 125.70 ($2CH_{Ar}$), 129.84 ($2CH_{Ar}$), 135.16 (CH_{Py}), 148.04 (CH_{Py}), 148.32 (CH_{Py}), 124.86, 135.58, 140.83, 154.52, 160.91, 169.63 ($6C_{quater}$); MS *m/z* (I_{rel}, %) 363.20 $[M+H]^+$ (100); Anal. calcd. for $C_{21}H_{22}N_4O_2$ (362.43): C, 69.83; H, 6.28; N, 15.31%; Found: C, 69.59; H, 6.12; N, 15.46%.

 doi:10.20944/preprints202405.1552.v1

3.2. In Vitro Biological Assays

Cell lines. The work was carried out on C6 glioma cell lines (rat) from the collection of the The Republican Research and Practical Center for Epidemiology and Microbiology (RRPCEM, Republic of Belarus).

Sample preparation. Test samples were dissolved in dimethyl sulfoxide (DMSO) to a concentration of 0.1 M. Then the resulting solution was diluted in an isotonic solution (0.9% sodium chloride solution) to a concentration of compounds of 2000 μM.

Solutions of the test compounds were added to the wells with cells in a volume of 10% of the total volume of the culture medium (in a ratio of 1 (test compounds) : 9 (medium with cells)). The final concentration of the test compounds is 200 μM, DMSO is 0.2%.

Antitumor drugs: cyclophosphamide (RUPE "Belmedpreparaty", Belarus), fluorouracil (RUPE "Belmedpreparaty", Belarus), etoposide (Fresenius Kabi, Germany), ribomustine (active substance - Bendamustine, Haupt Pharma Wolfratshausen GmbH, Germany), cisplatin (Pharmachemie B.V., Netherlands).

Conducting experiments. Cells were seeded into wells of 96-well plates (Corning) in DMEM (Sigma) supplemented with 10% fetal bovine serum (Sigma) and antibiotics (penicillin, streptomycin, neomycin, Biological Industries). The test compounds were added to the wells at a final concentration of 200 μM and/or antitumor drugs at a final concentration of 5 and 50 μM. In the control, instead of the tested compounds, a solvent dimethyl sulfoxide (DMSO), diluted in 0.9% sodium chloride, at a final concentration of 0.2% was added. Number of samples in each series n = 8. Cells were cultured for 48 hours at 37°C and 5% CO_2. Then the cells were removed from the plate and cell samples were prepared. To assess cell viability, cells were stained with 7-aminoactinomycin (7-AAD) or propidium iodide. To determine the total number of cells and the number of viable cells in the samples (as an end point characterizing the antitumor effect), FLOW-COUNT™ reference fluorospheres (Beckman Coulter) were used according to the manufacturer's instructions. Cellular samples were analyzed using a BD FACSCanto II flow cytometer (Becton Dickinson).

Statistical processing. The resulting digital material was processed by methods of variation statistics using the Excel and Statistica 7 software packages. The data are presented as the mean and its standard error. Differences between series were considered significant at a significance level of $p < 0.05$ according to Student's t test.

3.3. Quantum chemical methods.

The Gaussian 16 package software was used for DFT calculation and for visualization results of DFT calculation Gauss View 6.0.16 software was used. The calculations were performed within the framework of the DFT-D3 dispersion correction method [28], which, as shown in a number of works [29–31], is successfully used to take into account the inter- and intramolecular long-range dispersion interactions. The Becke's three-parameter exchange functional [32] in combination with the Lee et al. correlation functional [33] (B3LYP) were used. For reason this functional gives a high accuracy compared to experimental values for structures with intermolecular interactions, as demonstrated in [34,35].

Dunning's correlation consistent polarized valence double zeta basis set with adding diffuse functions aug-cc-pVDZ was used. Diffuse functions were added for describing long-range interactions such as Van der Waals forces and noncovalent interactions such as hydrogen bonding [36–38]. The LANL2DZ (Los Alamos National Laboratory 2 double zeta) basis set with effective core potential (ECP) was used for Pt [39].

Polarizable continuum model (PCM, solvent is considered as continuous dielectric medium) was used for solvent phase calculations [40]. The PCM model implements self-consistent reaction field (SCRF) approach and defines solvent polarization in terms of electrostatic potential. Following discussions are based on this method if not noted otherwise. No symmetric constraints were imposed during geometrical optimizations. The energy minima were identified by subsequent frequency calculations.

 doi:10.20944/preprints202405.1552.v1

3.4. Molecular docking

Molecular docking software packages AutoDock/Vina 4.2.6 and CHIMERA 1.16 was employed to calculate the protein–ligand binding interactions. The 3D crystal structure of the mouse thymidylate synthase (TS) was downloaded from the RCSB Protein Data Bank (PDB ID: 5FCT, 1.55 Å resolution). All bound waters ligands and cofactors were removed from the protein prior to the docking process. The protein was parameterized using AMBER f14SB force field. In order to include all the amino acid residues, the precalculated grid maps are set at the size of 65, 65 and 65 Å (x, y and z). Inhibition constant (K_i) of the docked compounds have been calculated from the docking score by applying the following formula: $K_i = \exp(\Delta G/RT)$, where ΔG denotes binding energy in Cal/mol, R denotes gas constant (1.987 Cal/mol-K), and T represents temperature in Kelvin (298,15 K). Intermolecular interactions between ligand and receptor protein were analyzed by BIOVIA Discovery Studio Visualizer 2024.

4. Conclusions

Taking into account the combination of theoretical calculations, molecular docking and test results, we can conclude:

In vitro tests of alkaloid-based isoxazolylureas on the C6 rat glioma model showed that a synergistic effect is observed to varying degrees for all studied compounds when using binary mixtures with alkylating chemotherapy drugs cisplatin and ribomustine, whereas antagonism and the tendency to antagonism are noted for the rest drugs, except for the combination with fluorouracil, where conflicting results have been observed.

The clear antagonistic effect of the combination of urea with cyclophosphamide, fluorouracil and etoposide resulting in 2-3 fold decrease of antiproliferative action can be explained based on the results of quantum chemical modeling of the spatial structure of the adjuvants. The structure of isoxazolylurea 2 differs from the other two in its most linear spatial arrangement, which could result in the varying degrees of conjugates stability. In addition, analysis of FMO localization in fluorouracil conjugates showed that HOMO and LUMO in contrast to cisplatin conjugates is completely localized on isoxazole heterocycle or alkaloid fragment but not on drug molecule. This means that the interaction with the electrophilic and nucleophilic regions of protein sites is realized mainly due to the adjuvant molecule.

Based on molecular docking data, all isoxazolyl ureas demonstrate a good binding degree to the thymidylate synthase protein site, forming an extensive system of residues interactions mainly due to the hydrophobic interactions of electron-rich π systems of isoxazole heterocycle and aromatic rings with amino acid residues which probably can confirms the possibility of competing binding processes with the thymidylate synthase site, but does not explain the synergy observed in the case of the composition of fluorouracil with anabasine isoxazolylurea 3. It is not excluded that ureas can be multitarget ligands that attack other proteins as well, and observed discrepant behavior of fluorouracil compositions should rather be explained by varying degrees of stability of drug-adjuvant complexes with the formation of an inactive product.

Isothiazolylurea adjuvants shape conjugates with cisplatin with non-covalent interactions between molecules due to hydrogen and van der Waals bonds generally forming more stable complexes than with fluorouracil. FMOs here are uniformly distributed between the adjuvant and the cisplatin molecule. It may indicate a coordinated mechanism of action cisplatin and the adjuvant in binary mixtures towards biological targets, which is confirmed by the experimentally observed synergistic effect.

The most pronounced synergistic effect was observed in the case of ribomustine mixtures with all synthesized compounds which encourages further research of the dose-dependent characteristics for this composition.

Supplementary Materials: The following supporting information can be downloaded at the website of this paper posted on Preprints.or

 doi:10.20944/preprints202405.1552.v1

Author Contributions: Conceptualization, G.K.M., V.A.K., V.I.P.; methodology, E.A.A., I.A.K., E.A.D., T.I.T.; investigation, E.A.A., I.A.K., E.A.D., T.I.T., A.L.P., D.A.L., D.L.M.; writing—original draft preparation, E.A.A., E.A.D., T.I.T., V.I.P., A.L.P.; writing—review and editing, G.K.M., R.I.J., A.Zh.S., M.S.N., A.R.Z., O.A.N., I.A.K.; project administration, G.K.M., V.I.P.; Software, E.A.A., A.L.P., D.A.L., D.L.M.; visualization, A.L.P., D.A.L., D.L.M.; supervision, G.K.M., V.I.P., V.A.K.; project administration, G.K.M. and V.I.P.; funding acquisition, G.K.M., R.I.J., A.Zh.S., M.S.N., A.R.Z., O.A.N. All authors have read and agreed to the published version of the manuscript.

Funding: The work was carried out within the framework of project No. AP19674667 with grant financing from the Science Committee of the Ministry of Science and Higher Education of the Republic of Kazakhstan and partly financial support from the Belarusian State Scientific Research Program "Convergence 2025", National Academy of Sciences of Belarus. D.L. and D.M. were partially supported by KAUST baseline funding.

Acknowledgments: All Gaussian16 computations were performed on KAUST's Ibex HPC, Saudi Arabia. The authors thank the KAUST Supercomputing Core Lab team for assistance with tasks execution on Skylake nodes.

Institutional Review Board Statement: Not applicable.

Informed Consent Statement: Not applicable.

Data Availability Statement: The data presented in this study are available in the article or supplementary material.

Conflicts of Interest: The authors declare no conflict of interest.

Sample Availability: Samples of the compounds are available from the authors.

References

1. Duarte, D.; Vale, N. Evaluation of synergism in drug combinations and reference models for future orientations in oncology. *Curr. Res. Pharmacol Drug Discov* **2022,** *3*, 100110.
2. Cheon, C.; Ko, S.G. Synergistic effects of natural products in combination with anticancer agents in prostate cancer: A scoping review. *Front Pharmacol* **2022**, *13*, 963317.
3. Gaston, T.E.; Mendrick, D.L.; Paine, M.F.; Roe, A.L.; Yeung, C.K. Natural is not synonymous with "Safe": Toxicity of natural products alone and in combination with pharmaceutical agents. *Regul Toxicol Pharmacol* **2020,** *113*, 104642.
4. Hackman, G.L.; Collins, M.; Lu, X.; Lodi, A.; DiGiovanni, J.; Tiziani, S. Predicting and Quantifying Antagonistic Effects of Natural Compounds Given with Chemotherapeutic Agents: Applications for High-Throughput Screening. *Cancers (Basel)* **2020**, *12(12)*, 3714.
5. Eid, A.M.; Hawash, M.; Amer, J.; Jarrar, A.; Qadri, S.; Alnimer, I.; Sharaf, A.; Zalmoot, R.; Hammoudie, O.; Hameedi, S.; Mousa, A. Synthesis and Biological Evaluation of Novel Isoxazole-Amide Analogues as Anticancer and Antioxidant Agents. *Biomed Res Int* **2021**, *2021*, 6633297.
6. Arya, G.C.; Kaur, K.; Jaitak, V. Isoxazole derivatives as anticancer agent: A review on synthetic strategies, mechanism of action and SAR studies. *Eur J Med Chem* **2021,** *221*, 113511.
7. Gupta, S.; Park, S.E.; Mozaffari, S.; El-Aarag, B.; Parang, K.; Tiwari, R.K. Design, Synthesis, and Antiproliferative Activity of Benzopyran-4-One-Isoxazole Hybrid Compounds. *Molecules* **2023**, *28*, 4220. https://doi.org/10.3390/molecules28104220
8. Zhu, J.; Mo, J.; Lin, H.; Chen, Y.; Sun, H. The recent progress of isoxazole in medicinal chemistry. *Bioorganic & Medicinal Chemistry* **2018**, *26(12)*, 3065
9. Kolesnik, I.A.; Kletskov, A.V.; Potkin, V.I., Knizhnikov, V.A.; Zvereva, T.D.; Kurman, P.V.; Tokalchik, Yu.P.; Kulchitsky, V.A. Glycylglycine and Its Morpholide Derivatives Containing 5-(p-Tolyl)isoxazole and 4,5-Dichloroisothiazole Moieties. *Russ J Org Chem* **2021**, 57, 1584
10. Kletskov, A.V.; Potkin, V.I.; Kolesnik, I.A.; Petkevich, S.K.; Kvachonak, A.V.; Dosina M.O.; Loiko D.O.; Larchenko M.V.; Pashkevich, S.G.; Kulchitsky, V.A. Synthesis and Biological Activity of Novel Comenic Acid Derivatives Containing Isoxazole and Isothiazole Moieties. *Natural Product Communications* **2018**, *13(11)*, 1507.
11. Potkin, V. I.; Petkevich, S. K.; Kletskov, A. V.; Zubenko, Y. S.; Kurman, P. V.; Pashkevich, S. G.; Kulchitskiy, V. A. The synthesis of isoxazolyl- and isothiazolylcarbamides exhibiting antitumor activity. *Russian Journal of Organic Chemistry* **2014**, *50(11)*, 1667
12. Potkin, V.; Pushkarchuk, A.; Zamaro, A.; Zhou, H.; Kilin, S.; Petkevich, S.; Kolesnik, I.; Michels, D.L.; Lyakhov, D.A.; Kulchitsky, V.A. Effect of the isotiazole adjuvants in combination with cisplatin in chemotherapy of neuroepithelial tumors: experimental results and modeling. *Sci Rep* **2023**, *13*, 13624

 doi:10.20944/preprints202405.1552.v1

13. Kulchitsky, V.A.; Potkin, V.I.; Zubenko, Y.S.; Chernov, A.N.; Talabaev. M.V.; Demidchik, Y.E.; Petkevich, S.K.; Kazbanov, V.V.; Gurinovich, T.A.; Roeva, M.O.; Grigoriev, D.G.; Kletskov, A.V.; Kalunov, V.N. Cytotoxic effects of chemotherapeutic drugs and heterocyclic compounds at application on the cells of primary culture of neuroepithelium tumors. *Medicinal Chemistry* **2012**, *8(1)*, 22-32
14. Giakoumettis, D.; Kritis, A.; Foroglou, N. C6 cell line: the gold standard in glioma research. *Hippokratia* **2018,** *22(3)*, 105
15. Dabbish, E.; Scoditti, S.; Shehata, M.N. I.; Ritacco, I.; Ibrahim, M.A.A., Shoeib, T.; Sicilia, E. Insights on cyclophosphamide metabolism and anticancer mechanism of action: A computational study. *J Comput Chem* **2024**, *45*, 663
16. Knüpfer, H.; Stanitz, D.; Preiss, R. CYP2C9 polymorphisms in human tumors. *Anticancer Res* **2006,** *26(1A)*, 299
17. Uthansingh, K.; Parida, P.K.; Pati, G.K.; Sahu, M.K.; Padhy, R.N. Evaluating the Association of Genetic Polymorphism of Cytochrome p450 (CYP2C9*3) in Gastric Cancer Using Polymerase Chain Reaction-Restriction Fragment Length Polymorphism (PCR-RFLP). *Cureus* **2022**, *14(7)*, e27220.
18. Khan, A.; Aldebasi, Y.H.; Alsuhaibani, S.A.; Khan, M.A. Thymoquinone Augments Cyclophosphamide-Mediated Inhibition of Cell Proliferation in Breast Cancer Cells. *Asian Pac J Cancer Prev* **2019**, *20(4)*, 1153
19. Rivera-Lazarín, A.L.; Martínez-Torres, A.C.; de la Hoz-Camacho, R.; Guzmán-Aguillón, O.L.; Franco-Molinaa, M.A.; Rodríguez-Padilla, C. The bovine dialyzable leukocyte extract, immunepotent CRP, synergically enhances cyclophosphamide-induced breast cancer cell death, through a caspase-independent mechanism. *EXCLI J.* **2023**, *22*, 131
20. Dewidar, S.A.; Hamdy, O.; Soliman, M.M.; El Gayar, A.M.;, El-Mesery, M. Enhanced therapeutic efficacy of doxorubicin/cyclophosphamide in combination with pitavastatin or simvastatin against breast cancer cells. *Med. Oncol.* **2023,** *41(1)*, 7
21. Zhang, N.; Yin, Y.; Xu S.J.; Chen, W.S. 5-Fluorouracil: mechanisms of resistance and reversal strategies. *Molecules* **2008**, 13(8), 1551
22. Azwar, S.; Seow, H.F.; Abdullah, M.; Faisal Jabar M.; Mohtarrudin, N. Recent Updates on Mechanisms of Resistance to 5-Fluorouracil and Reversal Strategies in Colon Cancer Treatment. *Biology (Basel)* **2021**, *10(9)*, 854.
23. Siddiqui, M.F.; Muqaddas, M.; Sarwar, S. Biochemical mechanisms of etoposide; upshot of cell death. *IJPSR* **2015**, *6(12)*, 4920
24. Dasari, S.; Tchounwou, P.B. Cisplatin in cancer therapy: molecular mechanisms of action. *European Journal of Pharmacology* **2014**, *740*, 364
25. Gandhi, V. Metabolism and mechanisms of action of bendamustine: Rationales for combination therapies. *Seminars in Oncology* **2002**, 29(4), 4
26. Richards, R.; Schwartz, H.R.; Honeywell, M.E.; Stewart, M.S.; Cruz-Gordillo, P.; Joyce, A.J.; Landry, B.D.; Lee, M.J. Drug antagonism and single-agent dominance result from differences in death kinetics. *Nat. Chem. Biol.* **2020,** *16(7)*, 791.
27. Geerlings, P.; De Proft, F.; Langenaeker, W. Conceptual Density Functional Theory. *Chem. Rev.* **2003**, *103*(5), 1793
28. Grimme, S.; Antony, J.; Ehrlich, S.; Krieg, H. A consistent and accurate ab initio parametrization of density functionaldispersion correction (DFT-D) for the 94 elements H-Pu. *J. Chem Phys.* **2010**, *132 (15)*, 154104
29. Grimme, S.; Hansen, A.; Brandenburg, J.G.; Bannwarth, C. Dispersion-Corrected Mean-Field Electronic Structure Methods. *Chem. Rev.* **2016**, *116*, 5105
30. Goerigk, L.; Hansen, A.; Bauer, C.; Ehrlich, S.; Najibi, A.; Grimme, S. A look at the density functional theory zoo withthe advanced GMTKN55 database for general main group thermochemistry, kinetics and noncovalent interactions. *Phys.Chem.Chem.Phys.* **2017**, *19*, 32184
31. Raju, R.K.; Bengali, A.A.; Brothers, E.N. A unified set of experimental organometallic data used to evaluate modern theoretical methods. *Dalton Trans.* **2016**, *45*, 13766
32. Becke, A.D. Density-functional thermochemistry. III. The role of exact exchange. *Journal of Chemical Physics* **1993**, *98*, 5648
33. Lee, C.; Yang, W.; Parr, R.G. Development of the Colle-Salvetti correlation-energy formula into a functional of the electron density. *Physical Review B* **1988**, *37*, 785
34. Makrlik, E.; Toman, P.; Vanura, P. A combined experimental and DFT study on the complexation of Mg2+ with beauvericin E. *Structural Chemisty* **2012**, *23*, 765.
35. Fang, J.L.; Li, W.Z.; Zhou, J.; Chen, J.; Xia, C. Novel guanidinium zwitterion and derived ionic liquids: physicochemical properties and DFT theoretical studies. *Structural Chemistry* **2011**, *22*, 1119
36. Kendall, R. A.; Dunning, Jr. T. H.; Harrison, R. J. Electron affinities of the first-row atoms revisited. Systematic basis sets and wave functions. *J. Chem. Phys.* **1992**, *96*, 6796
37. Dunning, Jr. T. H. Gaussian basis sets for use in correlated molecular calculations. I. The atoms boron through neon and hydrogen. *J. Chem. Phys.* **1989**, *90*, 1007.

 doi:10.20944/preprints202405.1552.v1

38. Papajak, E.; Truhlar, D.G. Efficient Diffuse Basis Sets for Density Functional Theory. *J. Chem. Theory Comput.* **2010**, *6*, 597
39. Hay, P. J.; Wadt, W. R. Ab initio effective core potentials for molecular calculations. Potentials for K to Au including the outermost core orbitals. *J. Chem. Phys.* **1985**, *82*, 299.
40. Tomasi, J.; Mennucci, B.; Cammi, R. Quantum Mechanical Continuum Solvation Models. *Chem. Rev.* **2005**, *105*, 2999